Heterozygous splice mutation in *PIK3R1* causes human immunodeficiency with lymphoproliferation due to dominant activation of PI3K

Carrie L. Lucas,[1,2] Yu Zhang,[2,3] Anthony Venida,[1,2] Ying Wang,[5] Jason Hughes,[6] Joshua McElwee,[6] Morgan Butrick,[2,4] Helen Matthews,[1,2] Susan Price,[1,2] Matthew Biancalana,[1,2] Xiaochuan Wang,[5] Michael Richards,[7] Tamara Pozos,[8] Isil Barlan,[9] Ahmet Ozen,[9] V. Koneti Rao,[1,2] Helen C. Su,[2,3] and Michael J. Lenardo[1,2]

[1]Molecular Development of the Immune System Section, Laboratory of Immunology; [2]NIAID Clinical Genomics Program; [3]Human Immunological Diseases Unit, Laboratory of Host Defenses; and [4]Intramural Clinical Management and Operations Branch, National Institute of Allergy and Infectious Diseases, National Institutes of Health, Bethesda, MD 20892
[5]Department of Clinical Immunology, Children's Hospital of Fudan University, Shanghai 200433, China
[6]Merck Research Laboratories, Merck & Co, Boston, MA 02115
[7]Hematology/Oncology Clinic and [8]Infectious Diseases and Immunology, Children's Hospitals and Clinics of Minnesota, Minneapolis, MN 55404
[9]Pediatric Allergy and Immunology, Marmara University, Istanbul 34660, Turkey

Class IA phosphatidylinositol 3-kinases (PI3K), which generate PIP_3 as a signal for cell growth and proliferation, exist as an intracellular complex of a catalytic subunit bound to a regulatory subunit. We and others have previously reported that heterozygous mutations in *PIK3CD* encoding the p110δ catalytic PI3K subunit cause a unique disorder termed p110δ-activating mutations causing senescent T cells, lymphadenopathy, and immunodeficiency (PASLI) disease. We report four patients from three families with a similar disease who harbor a recently reported heterozygous splice site mutation in *PIK3R1*, which encodes the p85α, p55α, and p50α regulatory PI3K subunits. These patients suffer from recurrent sinopulmonary infections and lymphoproliferation, exhibit hyperactive PI3K signaling, and have prominent expansion and skewing of peripheral blood $CD8^+$ T cells toward terminally differentiated senescent effector cells with short telomeres. The *PIK3R1* splice site mutation causes skipping of an exon, corresponding to loss of amino acid residues 434–475 in the inter-SH2 domain. The mutant p85α protein is expressed at low levels in patient cells and activates PI3K signaling when overexpressed in T cells from healthy subjects due to qualitative and quantitative binding changes in the p85α–p110δ complex and failure of the C-terminal region to properly inhibit p110δ catalytic activity.

CORRESPONDENCE
Michael J. Lenardo:
lenardo@nih.gov

Abbreviations: CRP, C-reactive protein; ESR, erythrocyte sedimentation rate; EV, empty vector; HSCT, hematopoietic stem cell transplantation; IBD, inflammatory bowel disease; IVIG, intravenous immunoglobulin; LAT, linker of activated T cells; PASLI, p110δ-activating mutations causing senescent T cells, lymphadenopathy, and immunodeficiency; PI3K, phosphatidylinositol 3-kinase; WES, whole-exome sequencing.

Primary human immunodeficiency diseases offer insights into genes and pathways critical for host defense and healthy immune homeostasis. We and others have recently described a unique immune disorder featuring recurrent sinopulmonary infections, predisposition to chronic EBV and CMV viremia, lymphoproliferation, and increased lymphoma susceptibility (Angulo et al., 2013; Crank et al., 2014; Kracker et al., 2014; Lucas et al., 2014). Heterozygous gain-of-function mutations in the *PIK3CD* gene encoding the leukocyte-restricted p110δ catalytic subunit of phosphatidylinositol 3-kinase (PI3K) are responsible for this disorder, which we have termed p110δ-activating mutations causing senescent T cells, lymphadenopathy, and immunodeficiency (PASLI) disease (Lucas et al., 2014). PASLI disease is caused by mutation of at least four different sites in *PIK3CD* that drive hyperactivation of PI3K signaling in immune cells (Crank et al., 2014; Lucas et al., 2014). Some of the disease-causing amino acid substitutions in

The Rockefeller University Press $30.00
J. Exp. Med. 2014 Vol. 211 No. 13 2537–2547
www.jem.org/cgi/doi/10.1084/jem.20141759

Table 1. Clinical summary

Features	A.1	B.1	B.II.1	C.1
Demographics				
Age (years)	32	43	17	5
Gender	Female	Female	Male	Male
Ethnic background	Turkish	Caucasian American	Caucasian American	Chinese
Clinical Infections	Sinusitis, otitis, sinopulmonary, conjunctivitis	Otitis, sinopulmonary	Sinusitis, sinopulmonary, conjunctivitis	Sinopulmonary
Autoimmunity	Arthritis, IBD	Unknown	None	Arthritis
Cytopenias	Thrombocytopenia	Unknown	No	No
LAD	Yes	Yes	Yes	Yes
Splenomegaly	Yes; splenectomy	Yes	Yes; splenectomy	No
Pulmonary	Bronchiectasis	Unknown	Bronchiectasis	No
Inflammation	High ESR, CRP	Unknown	High ESR	High ESR, CRP
Other	Breast papillomas; poor growth	Recurrent lymphoma; HSCT	Cystic kidneys; poor growth	Hepatomegaly; sepsis; poor growth
PBMCs				
Lymphocyte ct	6,420/µl ↑	2,100/µl	1,312/µl	1,300/µl
T cell ct	4,488/µl ↑	Unknown	1,036/µl	1,144/µl
B cell ct	122/µl	Unknown	39/µl ↓	0.52/µl ↓
% CD4 T cell	16.8% ↓	Unknown	29% ↓	16.9% ↓
% CD8 T cell	50% ↑	Unknown	50% ↑	68.7% ↑
% B cell	1.9% ↓	Unknown	3% ↓	0.04% ↓
CD4:CD8	0.34 ↓	Unknown	0.58 ↓	0.25 ↓
Immunoglobulins				
IgG	↓ (on IVIG)	↓ (on IVIG)	↓ (on IVIG)	↓ (on IVIG)
IgA	<5 mg/dl ↓	Unknown	absent ↓	8 mg/dl ↓
IgM	1,646 mg/dl ↑	Unknown	36.9 mg/dl	14 mg/dl ↓
EBV/CMV	None	Unknown	CMV lymphadenitis	None

LAD: lymphadenopathy; ct: count; arrows indicate high and low values, respectively.

p110δ are identical to those occurring in tumor cells at homologous sites in *PIK3CA* encoding p110α, suggesting a similar molecular mode of action. Indeed, PASLI patients exhibit increased lymphoma risk that is further compounded by immunodeficiency leading to poor control of EBV viral loads (Crank et al., 2014; Kracker et al., 2014). We are now aware of ∼80 PASLI patients worldwide, and the number of patients diagnosed with this disorder is expected to increase. Our previous work clearly established that hyperactivation of the PI3K signaling pathway causes immune dysregulation and raised the question of whether or not mutations in other PI3K genes would cause similar clinical manifestations by augmenting this pathway.

The phosphoinositide 3-kinase (PI3K) pathway transduces cell growth and proliferation signals through generation of the PIP_3 second messenger, which is important for recruitment and activation of pleckstrin homology (PH) domain–containing signaling proteins. The class IA PI3K family members include the catalytic p110α, p110β, and p110δ proteins and the regulatory p85α, p55α, p50α, p85β, and p55γ proteins. The complex becomes activated upon recruitment to tyrosine-phosphorylated YXXM motifs with major signaling roles downstream of the insulin receptor, insulin-like growth factor-1 receptor, cytokine receptors, T cell receptor, and others. The class IA PI3Ks exist as a dimer of a catalytic and a regulatory subunit. The major roles of the regulatory subunit are to bind and stabilize p110 (Conley et al., 2012), inhibit p110 kinase activity (Burke et al., 2011), and recruit the PI3K complex to phosphotyrosine where binding of the SH2 domains to phosphotyrosine relieves the inhibitory (but not dimerizing) contacts with the catalytic subunit (Yu et al., 1998). There is debate about the existence and potential roles for free monomeric p85α that is not bound to p110 and its possible function in regulating PI3K activity (Geering et al., 2007b). Evidence against roles for free p85α includes the observation that monomeric p85α is relatively unstable (Brachmann et al., 2005; Zhao et al., 2006) and that p85α and p110 are obligate heterodimers normally present in the cell at 1:1 ratio (Geering et al., 2007a). Whether or not p85α can exist unbound to p110 and whether or not free p85α exerts biological or pathological effects remain open questions.

Studies in animal models have revealed a complex relationship between p110 and p85α (Vanhaesebroeck et al., 2005). The total *PIK3R1* knockout mouse dies in the perinatal

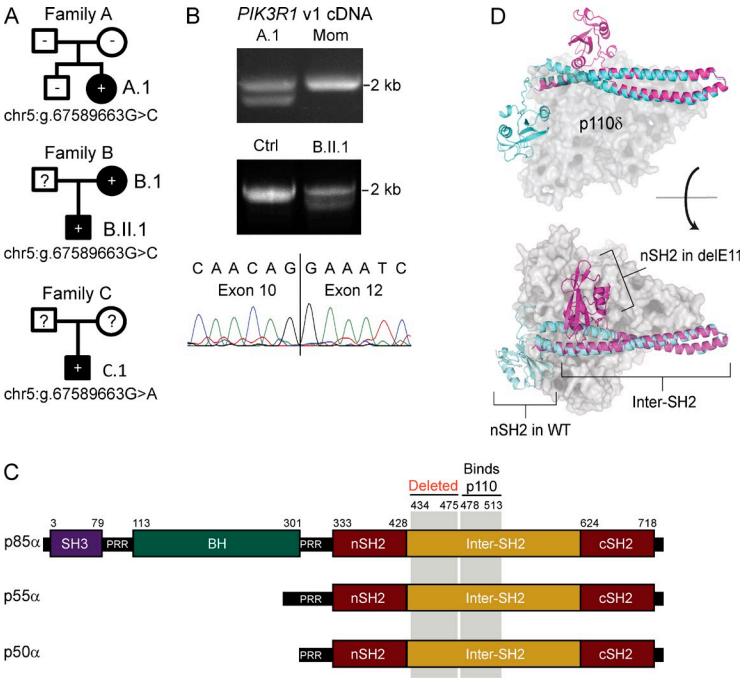

Figure 1. Affected patients are heterozygous for a *PIK3R1* splice site mutation that causes an in-frame deletion of exon 11. (A) Family pedigrees with clinically affected individuals in black and unaffected individuals in white. The mutation status is indicated within the symbol for each individual, where − indicates confirmed mutation-negative, + indicates confirmed mutation-positive, and ? indicates unknown mutation status. The specific nucleotide changes are indicated beneath each pedigree. (B) *PIK3R1* variant 1 cDNA (encoding p85α) amplified between exons 2 and 15 and imaged in an agarose gel (top) or sequenced using the Sanger approach after excision of the lower band (bottom). Three independent experiments on the two indicated patients and controls were performed. (C) Protein schematic for p85α, p55α, and p50α isoforms of *PIK3R1* indicating amino acid residue numbers (top), structural domains, region deleted by the patient splice mutation, and the p110-binding region. SH3: Src homology 3; PRR: proline-rich region; BH: breakpoint cluster region homology; nSH2 and cSH2: N-terminal and C-terminal Src homology 2. (D) Provisional structural model of the PI3K p85α protein showing an overlay of a WT (cyan) and delE11 (magenta) p85α protein fragment (nSH2 plus inter-SH2) in association with p110δ (gray). Top: view from side; Bottom: view from top.

period and shows secondary loss of p110 catalytic protein (Fruman et al., 2000). Mice heterozygous for p85α have normal levels of p110 and show greater insulin-stimulated PI3K activity than WT counterparts but display no overt immunological phenotypes (Ueki et al., 2002, 2003; Vanhaesebroeck et al., 2005). Two inherited human diseases have been associated with mutations in the *PIK3R1* gene: (1) SHORT syndrome, a disease of short stature, hyperextensible joints, Rieger anomaly of the eye, teething delay, lipoatrophy, and often insulin resistance, caused by heterozygous *PIK3R1* mutations (Chudasama et al., 2013; Dyment et al., 2013; Thauvin-Robinet et al., 2013; Bárcena et al., 2014); and (2) agammaglobulinemia due to absent B cells caused by a homozygous *PIK3R1* mutation that leads to loss of p85α with secondary loss of p110 (Conley et al., 2012). Somatic, heterozygous mutations in *PIK3R1* have also been found in human glioblastoma (Cancer Genome Atlas Research Network, 2008; Parsons et al., 2008) and colon cancer (Jaiswal et al., 2009). These mutations reduce inhibition of p110 by p85α, leading to hyperactive PI3K signaling and tumorigenesis (Jaiswal et al., 2009; Sun et al., 2010). More recently, somatic *PIK3R1* mutations in endometrial carcinoma were discovered that cluster mostly within amino acid residues 434–475 in the inter-SH2 domain of p85α and augment PI3K signaling (Urick et al., 2011). These findings in mice and previously described human diseases shed light on the various physiological roles of *PIK3R1* gene products and support the hypothesis that cancer-related *PIK3R1* gene mutations could be a driver of PASLI-like disease.

We have now discovered heterozygous *PIK3R1* splice site mutations in patients with PASLI-like disease characteristics and striking hyperactivation of PI3K signaling in immune cells. An independent report has also recently described similar patients with the same splice site mutation (Deau et al., 2014). Here, we not only describe the clinical findings and gene defect in these patients but also provide biochemical evidence that the mutant p85α protein is expressed in patient cells, associates abnormally with p110δ, and dominantly drives constitutive PI3K signaling due to loss of inhibitory contacts, which results in cellular derangements that contribute to immunodeficiency in this patient population. These findings further provide a possible treatment option for these patients using approved or investigational drugs that target PI3K or its downstream effectors (i.e., mTOR inhibition with rapamycin).

RESULTS

Immunodeficiency with poor antibody production, lymphoproliferation, and inflammatory disease

Our evaluation of the index patient A.1, a 32-yr-old female, revealed recurrent sinopulmonary infections with associated bronchiectasis, diffuse lymphadenopathy with splenomegaly, refractory immune thrombocytopenia purpura treated with splenectomy, and development of arthritis and inflammatory bowel disease (IBD) in adulthood (Table 1). Analysis of her blood cells revealed T lymphocytosis caused by expansion of CD8 T cells with normal CD4 T cell counts and normal or low B cell counts. Serum IgG levels were historically low in this patient, leading to treatment with intravenous immunoglobulin (IVIG) since the age of 6 yr. Serum IgA and IgM were low and high, respectively. Given her history of inflammatory arthritis and IBD, we evaluated markers of inflammation and found elevated erythrocyte sedimentation rate (ESR) and C-reactive protein (CRP). The patients in family B suffer from a similar disease with immunodeficiency, lymphoproliferation, and poor production of class-switched antibody. Patient B.1 developed Hodgkin lymphoma and has undergone hematopoietic stem cell transplantation (HSCT), and

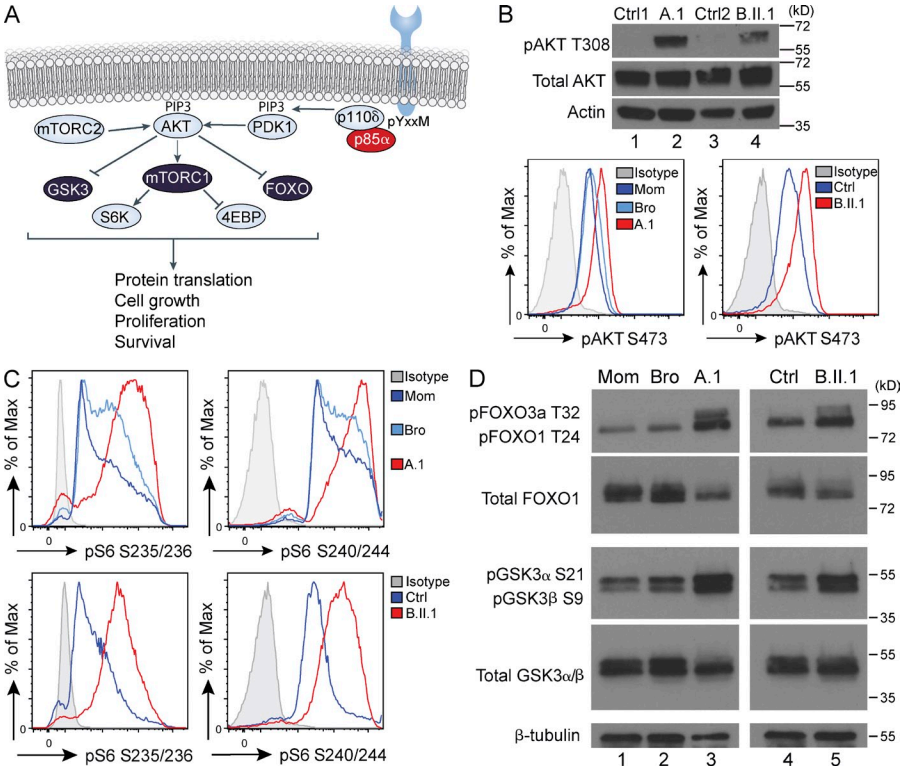

Figure 2. PI3K signaling is constitutively active in patient immune cells. (A) Signaling diagram showing the major molecules downstream of the p110δ/p85α PI3K complex. PDK1: phosphoinositide-dependent kinase-1; mTORC: mechanistic target of rapamycin complex; GSK3: glycogen synthase kinase 3; S6K: ribosomal protein S6 kinase; 4EBP1: eukaryotic translation initiation factor 4E-binding protein 1; FOXO: forkhead box O. (B) Immunoblot for AKT phosphorylated at threonine 308, total AKT, and actin (top), and flow cytometric analysis of AKT phosphorylation at serine 473 (bottom) in T cell blasts from healthy relatives or control subjects (Ctrl) and the indicated patients. (C) Flow cytometric analysis of the phosphorylation of S6 at serine residues 235/236 and serine residues 240/244 in T cell blasts from healthy relatives or control subjects (Ctrl) and the indicated patients (stained in same experiment as in B, bottom). (D) Immunoblot for phosphorylation of FOXO protein threonines (T) and GSK3 protein serines (S), total protein, or β-tubulin loading control, as indicated. Four (B and C) or three (D) independent experiments on the two indicated patients and controls were performed.

patient B.II.1 has been treated with IVIG since age 9, followed by Rituximab to deplete B cells starting at age 15. Patient C.1 is a young boy with immunodeficiency, lymphadenopathy, hepatomegaly, and severe juvenile rheumatoid arthritis. All patients have required IVIG supplementation and have a low CD4/CD8 ratio due to expansion of CD8 T cells.

Thus, the clinical features of this disease include immunodeficiency, lymphoproliferation, poor immunoglobulin responses, and expansion of CD8 T cells with susceptibility to inflammatory disease. These findings fit the clinical picture of PASLI disease (Lucas et al., 2014; also called activated p110δ syndrome; Angulo et al., 2013) caused by p110δ hyperactivation. However, mutations in the *PIK3CD* gene encoding p110δ were not found in the individuals described above, leading to the hypothesis that a mutation in another PI3K gene could be responsible for their disease.

Heterozygous splice site mutation in *PIK3R1* leads to in-frame loss of exon 11 and corresponding deletion of amino acid residues 434–475 in the inter-SH2 domain

The three families in our cohort demonstrate a dominant or de novo disease inheritance pattern, and whole-exome sequencing (WES) uncovered a heterozygous point mutation in *PIK3R1* at a splice donor site (G > C or G > A at chr5:67589663, which corresponds to c.1425+1 in NM_181523.2) in genomic DNA from PBMCs in patients A.1, B.II.1, and C.1 (Fig. 1 A). Due to her HSCT, genomic DNA was isolated from fingernail clippings from patient B.1 to confirm the presence of the mutation. The *PIK3R1* mRNA variant encoding p85α contains 16 exons beginning with a noncoding exon 1 in the 5′ UTR, and the patient splice site mutation is in the first intronic nucleotide after exon 11. The mutation results in skipping of exon 11 (delE11), as revealed by sequencing of *PIK3R1* cDNA (Fig. 1 B). As previously reported (Deau et al., 2014), loss of exon 11 led to an in-frame deletion of the nucleotides encoding amino acid residues 434–475 of p85α, which falls in the inter-SH2 domain shared by the p85α, p55α, and p50α *PIK3R1* isoforms (Fig. 1 C). This deletion is immediately N-terminal to the mapped binding site (residues 478–513) of the p110 catalytic subunit (Dhand et al., 1994). Structural modeling of the truncated inter-SH2 domain showed loss of part of the coiled coil structure of the inter-SH2 domain and predicted a dramatic change in the position of the nSH2 (positioned in the lower left in WT and shifted to the top in delE11) and cSH2 domains that are required for inhibitory contacts with p110 and recruitment to phosphotyrosine motifs (Fig. 1 D). Such a marked alteration in the inter-SH2 domain and the positioning of the SH2 domains strongly suggests that there will be qualitative and/or quantitative alterations in the contacts made between delE11 p85α and the p110 catalytic subunit. Moreover, all three *PIK3R1* gene products, the p85α, p55α, and p50α regulatory subunits, will be affected by this structural alteration that is predicted to impair p110 inhibition (Fig. 1 C).

PI3K signaling is hyperactive and constitutive

We next sought to directly examine PI3K signaling in these patients. PI3K activity generates PIP_3 to activate several downstream signaling pathways via the AKT serine/threonine kinase, which is recruited to the membrane at signaling sites by binding

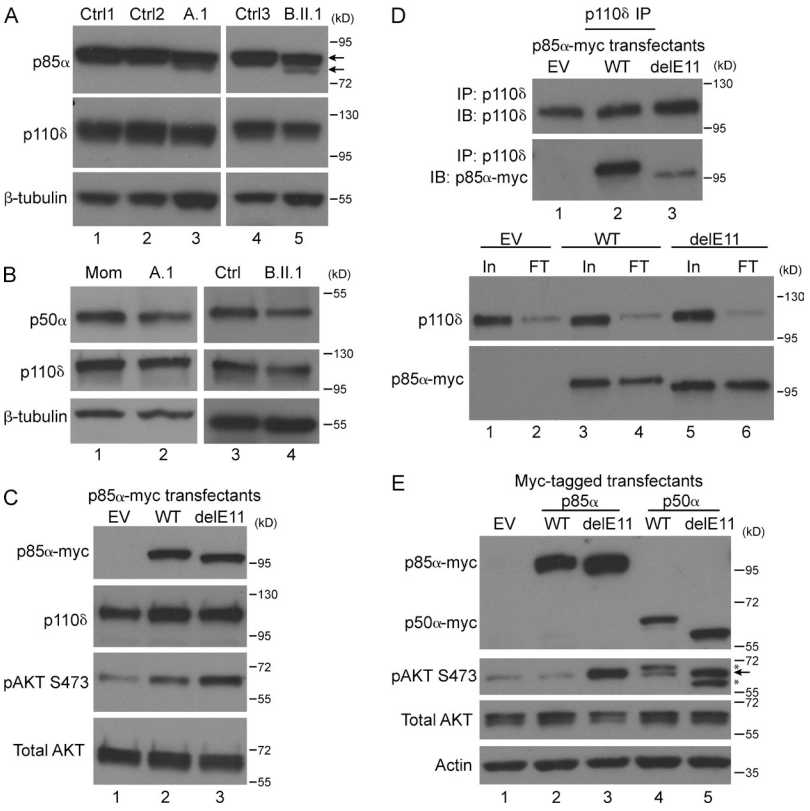

Figure 3. The delE11 *PIK3R1* mutant p85α gene product is expressed at low levels in patient T cell blasts and drives PI3K hyperactivation via poor inhibition of p110δ. (A) Western blot for p85α (Ab recognizing region just after SH3 domain), p110δ, or β-tubulin, as indicated. Arrows point to full-length (top arrow) and truncated delE11 (bottom arrow) p85α. (B) Western blot analysis of p50α using an antibody recognizing the N-terminal SH2 (top). Levels of p110δ protein (middle) and β-tubulin loading control (bottom) are also shown. (C) Primary T cells overexpressing EV, WT, or delE11 mutant 5x-myc-tagged p85α were analyzed by immunoblot for myc tag, p110δ, phospho-AKT, or total AKT, as indicated. (D) p110δ immunoprecipitates (IP, top) or input (In) and flow-through (FT; bottom) from T cells overexpressing EV, WT p85α-myc, or delE11 p85α-myc were probed with the indicated immunoblot (IB) antibodies. (E) Primary T cells overexpressing EV, WT, or delE11 mutant 5x-myc-tagged p85α or p50α were analyzed by immunoblot for myc tag, phospho-AKT, total AKT, or actin, as indicated. Arrow marks phospho-AKT band, and asterisks mark residual signal from p50α-myc blot reprobed for phospho-AKT. Four (A and C) or three (B, D, and E) independent experiments were performed.

to PIP_3 through its PH domain. Once active, AKT phosphorylates the GSK3α/β, mTOR, and FOXO1/3 proteins to promote protein translation, cell growth, proliferation, and survival (Fig. 2 A). We directly examined PI3K signaling in patient T cell blasts by evaluating AKT phosphorylation on threonine 308 and serine 473 and found substantially more basal phospho-AKT in patient samples compared with controls (Figs. 2 B). Also consistent with augmented PI3K signaling, phosphorylation of S6 at serine residues 235/236 and serine residues 240/244 was constitutively increased in patient T cell blasts compared with controls (Fig. 2 C). Finally, phosphorylation of FOXO1/3a (T24/T32) and GSK3α/β (S21/9) was similarly augmented in patients compared with controls (Fig. 2 D). Thus, the heterozygous *PIK3R1* mutations in these patients promote pathological, constitutive hyperactivation of PI3K and AKT, which leads to activation of the mTORC1 complex and phospho-inhibition of GSK3α/β and FOXO1/3.

The mutant p85α protein is detectable at low levels in patient T cell blasts and drives PI3K hyperactivation due to altered interaction with p110δ

We next sought to examine expression of the mutant p85α protein to determine if the in-frame deletion produces a stable protein product. Detection of endogenous p85α by immunoblot in lysates from patient T cell blasts revealed a reduction in full-length p85α compared with controls (Fig. 3 A). Importantly, a band at the predicted size of 78 kD was detectable in patient lanes (Fig. 3 A, bottom arrow). However, the truncated delE11 mutant form of p50α was undetectable (Fig. 3 B). The low-level mutant p50α protein expression despite the clear mRNA expression (unpublished data) suggests that the mutant protein is unstable. Examination of PI3K signaling after siRNA-mediated knockdown of *PIK3R1* showed no evidence for haploinsufficiency of *PIK3R1* contributing to hyperactivation of PI3K in primary human T cells (unpublished data). Moreover, we observed normal expression of the PTEN and SHIP1 phosphatases in patient T cell blasts, excluding the possibility that reduction in expression of the enzymes that counteract PI3K accounted for increased signaling (unpublished data). We next performed overexpression experiments in which WT versus delE11 5x-myc–tagged p85α was ectopically expressed in T cells from a healthy control subject and found that the mutant exerted a dominant, gain-of-function effect on PI3K signaling, causing increased AKT serine 473 phosphorylation (Fig. 3 C, compare lanes 1 and 3). We further found that WT and delE11 p85α-myc were similarly recruited to linker of activated T cells (LAT), a protein known to recruit p85α upon tyrosine phosphorylation (unpublished data).

Because the deletion removes residues near the p110-binding site, we next determined whether or not delE11 p85α associates normally with p110δ. To test this, we overexpressed myc-tagged WT or delE11 p85α in T cells from a healthy control subject and immunoprecipitated p110δ from cell lysates. The p110δ catalytic subunit strongly associated with myc-tagged WT p85α but exhibited reduced association with myc-tagged delE11 p85α despite robust expression in the input lysate (Fig. 3 D). Impaired association with p110δ offers a possible explanation for the reduced expression of

delE11 p85α in patient cells because the p85α monomer has been shown to be unstable (Brachmann et al., 2005; Zhao et al., 2006). These data, together with the observation that p110δ protein levels are relatively normal in these patients, indicate that the delE11 p85α protein expressed in patient cells can associate with p110δ and stabilize it, though the affinity of the interaction is reduced compared with WT because the complexes fail to remain intact in immunoprecipitation procedures.

The experiments above shed light on the stability of the association between p85α and p110δ, which dimerize via stable contacts mediated by the inter-SH2 domain of p85α and the adaptor-binding domain of p110δ. However, the data above do not address the additional inhibitory contacts normally made between the SH2/inter-SH2 domains of p85α and various regions of p110δ. We assessed the contribution of the SH2/inter-SH2 domains of the delE11 p85α mutant in driving PI3K signaling by overexpressing myc-tagged p50α protein containing only these domains. When WT and delE11 forms of the C-terminal p50α fragment were overexpressed, we observed that delE11 p50α was sufficient to increase AKT phosphorylation on serine 473 (Fig. 3 E). These data rule out a role for the N-terminal domains (i.e., the SH3, PRR, and BH domains) of p85α in mediating the dominant gain-of-function effect on PI3K activity and instead point to a failure of delE11 p85α to inhibit p110δ activity due to alterations in the structure of the SH2 and inter-SH2 domains that normally form inhibitory contacts with the p110 subunit. Thus, the heterozygous *PIK3R1* splice mutation results in expression of mutant p85α that is sufficient to dominantly hyperactivate the PI3K pathway due to qualitatively and quantitatively different binding and impaired inhibition of p110δ.

Patient PBMCs are enriched with CD8 T cells that are terminally differentiated and have shortened telomeres

Because the *PIK3R1* mutation in these patients drives PI3K signaling, we expected to see similar cellular derangements as previously observed in PASLI patients with gain-of-function mutations in *PIK3CD* encoding p110δ. We therefore evaluated patient PBMCs and found several of the key cellular features of PASLI disease. CD8 T cells were increased in frequency and deficient in naive ($CD45RA^+CCR7^+$) cells with overrepresentation of CCR7-negative effector-type T cells in PBMCs from patients compared with controls (Fig. 4 A). T cell activation, as measured by CD25 up-regulation, was normal after stimulation of PBMCs with anti-CD3 and anti-CD28 (unpublished data). We next evaluated glucose uptake in T cell blasts using a fluorescent glucose analogue and found, as observed for PASLI patients with *PIK3CD* mutations, an increase in glucose uptake by T cell blasts from *PIK3R1* patients compared with controls (Fig. 4 B). Moreover, the majority of patient CD8 T cells were $CD57^+$, indicating terminal differentiation and senescence of the CD8 T cell population (Fig. 4 C). To extend these cellular findings, we assessed telomere length in the lymphocyte population by flow cytometry–based fluorescence in situ hybridization (flow-FISH) and

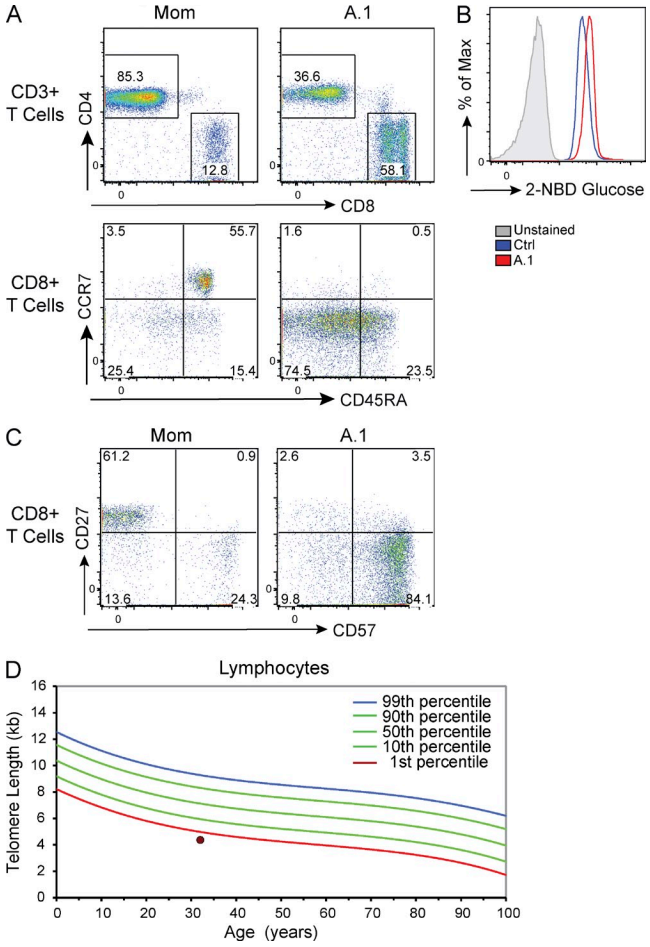

Figure 4. Patient CD8 T cells are expanded, severely skewed toward effector (CCR7-negative) phenotype, and enriched with senescent $CD57^+$ cells with short telomeres. (A) Flow cytometric analysis of PBMCs from a healthy control subject (Mom) or patient A.1, staining for CD4, CD8, CD45RA, and CCR7, as indicated. (B) Glucose uptake in the indicated T cell blasts, as measured by 2-NBDG (2-(N-(7-Nitrobenz-2-oxa-1,3-diazol-4-yl)Amino)-2-Deoxyglucose) fluorescence after a 1-h rest in PBS and 20-min incubation with 2-NBDG. (C) Flow cytometric analysis of PBMCs, gating on CD8 T cells, and assessing expression of CD57 and CD27. (D) Flow-FISH analysis of telomere length within the lymphocyte population in patient A.1 shown as a dot with percentiles indicated (courtesy of Repeat Diagnostics). Three (A, B, and C) or two (D, patients A.1 and B.II.1) independent experiments were performed.

observed severely shortened telomere length in *PIK3R1* patients (Fig. 4 D). Thus, in *PIK3R1*-driven disease as in p110δ PASLI disease, hyperactive PI3K signaling in lymphocytes causes expansion, terminal differentiation, and senescence of CD8 T cells.

The p110δ catalytic subunit accounts for hyperactivation of PI3K signaling and its inhibition offers potential for therapeutic benefit

To further validate our hypothesis that the *PIK3R1* mutation underlies the disease pathogenesis in these patients and causes hyperactivation of PI3K and mTOR in lymphocytes, we next

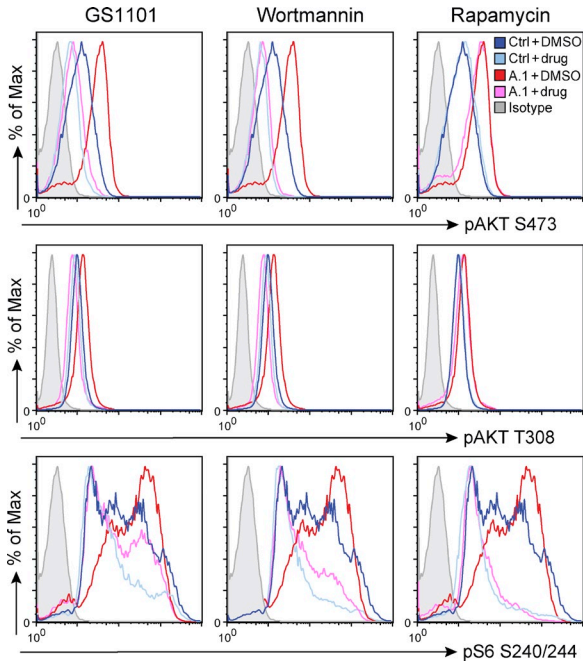

Figure 5. Targeted inhibition of mTOR or p110δ represent potentially effective treatment options for *PIK3R1* patients. Flow cytometric histograms for T cell blasts from healthy control subjects (Ctrl) or patient A.1 after treatment with 0.1 µM GS1101, 0.1 µM Wortmannin, or 12.5 nM rapamycin and analyzed for phosphorylation of AKT and S6 at the indicated residues. Four independent experiments were performed.

tested the effect of inhibiting these kinases in patient T cell cultures. As expected, inhibition of mTOR with rapamycin clearly reduced S6 phosphorylation but not AKT phosphorylation, whereas treatment of patient cells with GS1101, an FDA-approved p110δ-specific inhibitor, or Wortmannin, a pan-PI3K inhibitor, efficiently reduced both AKT and S6 phosphorylation (Fig. 5). The observation that the hyperactive PI3K pathway in patient T cell blasts was inhibited equally well by p110δ-specific inhibition and broader inhibition of all class IA PI3K catalytic subunits suggests that p110δ accounts for most or all of the hyperactive PI3K signaling in T cell blasts, which also express p110α and p110β. This finding raises the interesting possibility that delE11 p85α has unique effects on p110δ relative to other catalytic subunits and may help to explain why the clinical phenotype of *PIK3R1* patients involves effects mainly in the immune system. Moreover, these findings suggest treatment options for these patients using rapamycin or p110δ-specific inhibitors.

DISCUSSION

The PI3K signaling pathway plays critical roles in virtually all cell types and has been intensively studied because of its prominent role in promoting tumorigenesis. It has become clear that either too little or too much PI3K signaling can be pathological. Mice completely deficient in the *PIK3R1* gene products die in the perinatal period and exhibit liver necrosis and hypoglycemia, whereas mice lacking just the p85α isoform are viable but suffer from hypoglycemia and increased insulin sensitivity linked to up-regulation of the p55α and p50α isoforms (Fruman et al., 2000). Hyperactivation of PI3K signaling has been identified as a cause of human diseases including megalencephaly syndromes (Lee et al., 2012; Rivière et al., 2012) and overgrowth syndromes (Lindhurst et al., 2012; Keppler-Noreuil et al., 2014). A vast literature also places PI3K among the top pathways driving cancer cell growth and survival through gain-of-function mutation of PI3K genes, most commonly *PIK3CA* encoding the p110α catalytic subunit, or mutations activating upstream initiators of PI3K signaling (Wong et al., 2010).

Although most studies of PI3K signaling in disease states focus on the catalytic subunit, recent reports have clearly highlighted the important role that the regulatory subunit can play in modulating PI3K activity. Recently, several independent groups have identified heterozygous mutations in *PIK3R1* in patients with SHORT syndrome, a rare disorder characterized by short stature, hyperextensible joints, ocular depression, Rieger anomaly of the eye, teething delays, and characteristic facial gestalt (Chudasama et al., 2013; Dyment et al., 2013; Thauvin-Robinet et al., 2013; Bárcena et al., 2014). The *PIK3R1* mutations in these patients cluster predominantly in the cSH2 domain and the biochemical effect of these heterozygous mutations appears to be a reduction in insulin-stimulated PI3K activity (Chudasama et al., 2013; Dyment et al., 2013; Thauvin-Robinet et al., 2013; Bárcena et al., 2014). No severe immune abnormalities have been reported in patients with SHORT syndrome, and the clinical features of SHORT syndrome are not found in our *PIK3R1* patients with PASLI-like immune disease. These observations raise the possibility that the C-terminal SH2 domain of p85α plays a unique role in binding tyrosine-phosphorylated insulin receptor substrate-1 (IRS-1) during insulin signaling, leading to SHORT syndrome when mutated. In contrast, the N-terminal SH2 and inter-SH2 domains of p85α appear to be particularly important in inhibiting catalytic activity of p110δ because their alteration in our heterozygous *PIK3R1* patients causes PASLI-like immune disease via hyperactivation of p110δ.

Other *PIK3R1* findings particularly relevant for the studies described here are reports describing patients with homozygous loss of p85α (Conley et al., 2012) and tumors with heterozygous gain-of-function *PIK3R1* variants that augment PI3K signaling (Jaiswal et al., 2009; Sun et al., 2010; Urick et al., 2011). Conley et al. (2012) described a patient with colitis and absent B cells with normal T cells who harbored a homozygous loss-of-function mutation in *PIK3R1* resulting in absence of p85α protein with normal expression of the p50α and p55α splice variants. The mutation results in a premature stop codon in the BH domain that is present in the p85α but not the p55α or p50α isoforms of *PIK3R1*. Due to the lack of the regulatory p85α protein, a loss in expression of the catalytic p110δ subunit was observed, emphasizing the requirement for p85α to stabilize p110δ even when p55α and p50α are present. Interestingly, loss of p85α led to a dramatic decrease in p110δ with a more subtle decrease in expression of p110α and p110β (Conley et al., 2012). Thus, p85α/p110δ are required for B cell development, and the

N-terminal region of p85α plays a particularly important role in stability of p110δ (more so than the other class IA catalytic subunits). The heterozygous parents of this patient were not reported to be clinically affected, providing further support that haploinsufficiency of p85α is not a driver of PI3K hyperactivation in the immune system. In contrast to p85α loss of function, heterozygous mutations in *PIK3R1* that drive hyperactivation of PI3K have been identified in human cancers and found to have no effect on p110 protein expression levels (Jaiswal et al., 2009; Sun et al., 2010; Urick et al., 2011). In endometrial cancer, these mutations cluster in the inter-SH2 domain of p85α around amino acid residues 434–475, which are precisely the residues deleted by skipping of exon 11 in our patients, and the *PIK3R1* mutants drive hyperactivation of PI3K signaling (Urick et al., 2011).

Here, we describe patients who suffer from immunodeficiency with lymphoproliferation, antibody defects, and terminal differentiation and senescence of CD8 T cells. We identified a heterozygous splice site mutation that leads to in-frame deletion of exon 11 of *PIK3R1* and hyperactivation of PI3K and AKT. Similar patients with the same splice site mutation have now been independently reported (Deau et al., 2014). As in Deau et al. (2014), we describe a similar patient phenotype, mutation site, exon skipping, hyperphosphorylation of AKT and S6, and ability of overexpressed delE11 p85α to induce hyperphosphorylation of AKT. We further show that other AKT substrates including FOXO and GSK3 proteins are hyperphosphorylated in patient T cells. Most of the clinical features of the disease observed in our patients and those reported by Deau et al. (2014) are consistent, with lymphoproliferation and autoimmune/inflammatory disease being the two exceptions. We observed marked lymphoproliferation and reduced CD4/CD8 ratios in our patients, whereas only one of four patients reported by Deau et al. (2014) is reported to have evidence of lymphoproliferation (enlarged tonsils) and two of four patients have reduced CD4/CD8 ratios. Additionally, two of our four patients had arthritis, whereas none was reported by Deau et al. (2014). In both patient cohorts, recurrent sinopulmonary infections, immunoglobulin defects, and reduction in naive T cells are key characteristics of the disease. The molecular basis of PI3K hyperactivation and metabolic effects of cellular phenotype were not elaborated in Deau et al. (2014). We now report the mechanism by which deletion of amino acid residues 434–475 of p85α augments PI3K signaling and alters T cell phenotype and function, and our major conclusions are discussed below.

Normal T cells robustly express the p85α and p50α isoforms but not the p55α isoform of *PIK3R1*. Analysis of patient T cell lysates by immunoblot for *PIK3R1* protein products using an antibody against the nSH2 domain revealed, as expected, that full-length WT p85α and p50α were reduced in protein abundance. A truncated delE11 p85α band was observed at the expected size of 78 kD; however, the delE11 p50α mutant protein could not be detected despite clear mRNA expression (unpublished mRNA data). These observations left open the possibilities of gain-of-function effects on PI3K signaling mediated by low-level expression of delE11 p85α or a haploinsufficiency effect due to the reduction in expression of full-length WT p85α and p50α. Although haploinsufficiency of *PIK3R1* has been shown previously to increase PI3K signaling in response to insulin (Mauvais-Jarvis et al., 2002), we ruled out a major contribution of *PIK3R1* haploinsufficiency in this immune cell phenotype using siRNA-mediated knockdown of *PIK3R1* in T cells from healthy control subjects. These experiments showed no effect on levels of basal AKT phosphorylation, which is consistent with previous reports that insulin signaling is unique in its hyperresponsiveness caused by *PIK3R1* haploinsufficiency (Vanhaesebroeck et al., 2005). In contrast, when delE11 p85α was overexpressed in control T cells, we observed a clear increase in basal AKT phosphorylation relative to the WT p85α transfectants. This finding supports the conclusion that expression of the delE11 variant of p85α in patient immune cells is a dominant driver of PI3K hyperactivation.

To understand how delE11 p85α drives exuberant PI3K signaling, we examined the ability of this mutant protein to associate with the p110δ catalytic subunit because the deleted exon encodes residues adjacent to the p110 binding site. These experiments demonstrated a detectable but reduced association between endogenous p110δ and overexpressed delE11 p85α, whereas the association with overexpressed WT p85α was robust. This reduced association offers an explanation for the low-level expression of delE11 p85α in patient lysates because p85α is unstable if not bound to p110 (Brachmann et al., 2005; Zhao et al., 2006). How can delE11 p85α promote p110δ hyperactivation despite less stable interaction with p110δ? We evaluated three major possibilities: (1) structural effects of the deletion result in increased recruitment of the PI3K complex to phosphotyrosine; (2) delE11 p85α that is free from p110 interacts with other signaling molecules via its N-terminal SH3 domain, proline-rich regions, and/or BH domain to promote PI3K activity; and/or (3) the ability of delE11 p85α to form inhibitory contacts with p110δ is impaired. To address (1), we evaluated association of myc-tagged WT or delE11 p85α with LAT, which recruits p85α once it is tyrosine phosphorylated upon TCR engagement, and found that WT and delE11 p85α were similarly associated with LAT (unpublished data). We next addressed possibilities (2) and (3) by cloning and overexpressing the C-terminal fragment of WT and delE11 p85α containing only the nSH2, inter-SH2, and cSH2 domains (i.e., p50α) that normally form inhibitory contacts with p110. In T cells from healthy subjects, we found that overexpression of delE11 p50α was sufficient to cause hyperphosphorylation of AKT at serine 473. This result rules out a requirement for the N-terminal SH3, PRR, and/or BH domains of "free" delE11 p85α in promoting PI3K activity. Instead, our findings are consistent with a failure of the SH2 and inter-SH2 domains of delE11 p85α to properly inhibit p110δ due to structural derangements that interfere with formation of inhibitory contacts.

We now recognize two classes of PASLI disease distinguished by the gene underlying hyperactive PI3K signaling. We term these classes PASLI-CD and PASLI-R1 for the forms

caused by mutations in *PIK3CD* and *PIK3R1*, respectively. The clinical and cellular consequences of hyperactive PI3K signaling in immune cells were revealed by studies of PASLI-CD patients harboring heterozygous, gain-of-function mutations in *PIK3CD* encoding p110δ (Angulo et al., 2013; Lucas et al., 2014). The clinical presentations of the PASLI-R1 patients described here and in a recently published report (Deau et al., 2014) are remarkably similar to PASLI-CD patients, with recurrent sinopulmonary infections, poor antibody responses requiring IVIG, susceptibility to EBV and CMV, lymphoproliferation, and increased incidence of lymphoma. At the cellular level, we now show that, as in PASLI-CD patients, this new cohort of PASLI-R1 patients have increased glucose uptake, expanded CD8 T cells with significant reduction in the frequency of naive cells, and concomitant increase in the frequency of terminally differentiated effector-type T cells (Lucas et al., 2014). The CD57 senescence marker is also highly expressed on CD8 T cells in *PIK3R1* patients, and we extended this finding by determining that telomeres in lymphocytes are markedly shorter than expected for the age of the patient. Although presently these diseases appear to be very similar, following the natural history of these patients may reveal subtle clinical and/or molecular differences.

Given the molecular etiology of this disease, treatment with drugs inhibiting the PI3K signaling pathway would offer the most ideal therapeutic option for these patients. Indeed, we found that inhibition of mTOR using rapamycin in vitro robustly inhibited the hyperphosphorylation of S6 but had no effect on AKT hyperphosphorylation in PASLI-R1 T cell blasts. Because other targets of AKT besides mTOR (e.g., FOXO and GSK3α/β) are also hyperphosphorylated, a more ideal approach would be to specifically target select PI3K isoforms while avoiding negative consequences of global PI3K inhibition. Although T cells express all three class IA catalytic subunits, we were intrigued to find that inhibition of the leukocyte-restricted p110δ catalytic subunit alone was sufficient to reduce the hyperphosphorylation of AKT and S6 in *PIK3R1* patient T cell blasts. This has the interesting biological implication of p85α-mediated regulation of p110δ being unique and selectively affected by loss of *PIK3R1* exon 11. Given these findings and the predominantly immunological clinical disease in these patients, specific targeting of p110δ using inhibitors such as those currently in clinical trials for hematological malignancy (Lannutti et al., 2011; Brown et al., 2014; Flinn et al., 2014; Gilbert, 2014; Kahl et al., 2014) offers a potentially safe and effective treatment option to restore immune homeostasis while limiting unwanted effects in nonimmune cells that do not express p110δ.

MATERIALS AND METHODS

Human subjects. All human subjects (or their legal guardians) in this study provided written informed consent in accordance with Helsinki principles for enrollment in research protocols that were approved by the Institutional Review Board of the National Institute of Allergy and Infectious Diseases, National Institutes of Health (NIH). Blood from healthy donors was obtained at the NIH Clinical Center under approved protocols. Mutations will be automatically archived by Online Mendelian inheritance in Man (OMIM) once the paper is published, and whole-exome data will be submitted in dbGaP. We will also create a webpage through National Center for Biotechnology Information (NCBI) to accumulate patient mutation data in the format of the Leiden Online Variant Database (LOVD) as patients are identified.

DNA sequencing. Genomic DNA was isolated from PBMC for proband A.1 and family members. SureSelect Human All Exon 50 Mb kit (Agilent Technologies) coupled with massively parallel sequencing by Illumina HiSeq Sequencing System was performed using the collected DNA. For individual samples, WES produced ~50–100× sequence coverage for targeted regions. Similar WES was also performed for patient B.II.1 and C.1. For confirmation of mutations in the patients, genomic DNA was PCR amplified and Sanger sequencing of purified PCR amplified products was performed. For cDNA preparation, total RNA was extracted from T cell blasts and cDNA was produced using an oligo-dT primer. The *PIK3R1* gene was amplified from the cDNA and the full-length and truncated bands were excised from an agarose gel for Sanger sequencing to detect joining of exon 10 with exon 12.

Whole-exome sequence analyses. All sequenced DNA reads were mapped to the hg19 human genome reference by Burrows-Wheeler Aligner with default parameters. Single nucleotide variant and indel calling were performed using the Genome Analysis Toolkit (the Broad Institute). All SNVs/indels were annotated by SeattleSeq Annotation and an in-house custom analysis pipeline was used to filter and prioritize for autosomal recessive or de novo disease-causal variants based on the clinical pedigree for patient A.1. For patient B.II.1 and C.1, the mutations were identified by targeted gene screening of the WES databased on the similarity of clinical phenotype in the cohort.

Protein structure modeling. The structure of the delE11 p85α N-SH2 and inter-SH2 domains was generated by manual editing of p85α coordinates obtained from the complex of p110α and p85α (PDB ID: 3HHM), which were regularized (i.e., disordered amino acids were interpolated) using SWISS-MODEL. The p85α N-SH2 domain and extant region of the coiled-coil domain were treated as rigid bodies, and were fused together by manual transposition of the SH2 domain to the new terminal residue of the coiled-coil. The relative orientations of the domains were then modified to resolve steric clashes with the cognate p110δ subunit of PI3K, modeled using I-TASSER and ModRefiner. All manual modeling and subsequent rendering was performed using PyMOL.

Cell culture and transfection. Human PBMCs were isolated by Ficoll-Paque PLUS (GE Healthcare) density gradient centrifugation, washed twice in PBS, and resuspended at 10^6 cells/ml complete RPMI 1640 (cRPMI) medium (Lonza) containing 10% FBS, 2 mM glutamine, and 100 U/ml each of penicillin and streptomycin (Invitrogen). Cells were activated with 1 μg/ml anti-CD3 (clone HIT3α; BD) and 1 μg/ml anti-CD28 (clone CD28.2; BD). After 3 d, activated T cells were washed and then cultured in complete RPMI-1640 medium supplemented with 100 U/ml recombinant human IL-2 (rhIL-2; R&D Systems). Transfection was performed with Amaxa Nucleofection kits (Lonza) for primary cells, using C-terminally 5×-myc-tagged constructs in pcDNA3.1.

Flow cytometry. For standard surface staining, PBMCs (10^6 cells/sample), sorted cells, expanded T cells, or cell lines were washed with PBS and incubated for 30 min at 4°C (dark) in 100 μl 5% FBS in PBS with indicated fluorochrome-labeled monoclonal antibodies or their isotype controls. After washing with PBS two times, 10,000-50,000 live cells were analyzed by flow cytometry. For phosflow staining, unless otherwise indicated, cells were kept in cRPMI while alive, fixed directly in cRPMI using Lyse/Fix (BD), and then permeabilized with perm buffer III (BD) according to manufacturer's instructions. The indicated antibodies were purchased from BD, eBioscience, BioLegend, or Cell Signaling Technology. For phosflow analyses, anti-pAKT S473 Alexa Fluor 647 (D9E; Cell Signaling Technology), anti-pAKT T308 Alexa Fluor 488 (C31E5E; Cell Signaling Technology), anti-pS6 S235/236 PE (N7-548; BD), and/or anti-pS6 S240/244 Alexa Fluor 647 (D68F8; Cell Signaling Technology) were used. Rabbit isotype control staining was performed for each experiment (Fig. 2, B, left, with Fig. 2 C, top; Fig. 2 B, right, with Fig. 2 C, bottom; and Fig. 5).

Immunoblotting and immunoprecipitation. Cells were washed in PBS or RPMI with no FCS and immediately lysed on ice in 1% Triton X-100, 50 mM Tris-Cl, pH 8, 150 mM NaCl, 2 mM EDTA, 10% glycerol, complete protease inhibitor cocktail (Roche), and phosphatase inhibitor cocktails (Sigma-Aldrich). Protein was quantitated by BCA assay (Thermo Fisher Scientific). The lysates were then clarified by centrifugation at 15,000 *g* at 4°C for 10 min. Supernatants were transferred to a separate tube and used for subsequent experimentation. Approximately 20 µg of total protein was separated by SDS-PAGE and transferred to a nitrocellulose membrane (Bio-Rad Laboratories). Membranes were blocked with 5% nonfat dry milk in Tris-buffered saline (TBS) with 0.01% Tween-20 (TBST) for 1 h at room temperature before incubating with primary antibody overnight at 4°C. After washing with TBST for 1 h at room temperature, HRP-conjugated secondary antibody was added for an additional hour at room temperature. After a final 1-h wash step, HRP substrate (Luminata Forte; Millipore) was added to the membranes, which were then subjected to chemiluminescent imaging. Validated primary antibodies were purchased from Cell Signaling Technology, Santa Cruz Biotechnology, Inc., or Millipore, and secondary antibodies were from SouthernBiotech. For immunoprecipitation (IP) of p110δ, cells overexpressing empty vector (EV), WT p85α-myc, or delE11 p85α-myc were lysed as described above, precleared of proteins that nonspecifically bind anti-rabbit IgG IP beads (Rockland Immunochemicals), and incubated overnight with rabbit anti-p110δ IgG (Santa Cruz Biotechnology, Inc.). Anti-rabbit IgG IP beads were then added to capture the immune complexes, and samples were rotated for 1 h at 4°C. Captured immune complexes were pelleted by centrifugation, washed three times with lysis buffer, and eluted by boiling after addition of SDS-containing sample buffer with reducing agent.

Glucose uptake. Cells were starved of glucose by incubation in PBS for 1 h before incubation with 100 µg/ml 2-deoxy-2-[(7-nitro-2,1,3-benzoxadiazol-4-yl)amino]-D-glucose (2-NBDG) for 20 min. Uptake was measured by flow cytometric evaluation of signal in the fluorescein channel.

Flow-FISH for telomere length assessment. Fresh blood from patient A.1 was shipped directly to Repeat Diagnostics for measurement of telomere length by flow cytometry, gating on either lymphocytes or granulocytes. A fluorescently labeled nucleic acid probe was used to hybridize with the TTAGGG repeats in telomeres, and fluorescence intensity provided a measure of telomere length. Telomere length measurements for patient lymphocytes and granulocytes were plotted relative to telomere lengths established for healthy control subjects with percentiles indicated.

The authors thank the referring physicians as well as our patients and families who have gone to extraordinary efforts to join this study and provide samples. We also thank Deborah Rawson, Elaine Smoot, Julie Niemela, Jennifer Stoddard, and Dr. Sergio Rosenzweig for their important contributions to the clinical management of and laboratory medicine findings in these patients.

This research was supported by the Division of Intramural Research, National Institute of Allergy and Infectious Diseases and National Institutes of Health (NIH) Clinical Center, NIH. The work was also supported by Merck Inc., and we would like to thank Robert Plenge, Rupert Vessey, Dennis Zoller, Debbie Law, Huseyin Mehmet, and Ravi Ramadas for their support and collaboration. C.L. Lucas was supported by the Postdoctoral Research Associate (PRAT) Fellowship through the National Institute of General Medical Sciences. X. Wang and Y. Wang were supported by the National Natural Science Foundation of China (81172877, 81373221). The content of this publication does not necessarily reflect the views or policies of the Department of Health and Human Services, nor does mention of trade names, commercial products, or organizations imply endorsement by the U.S. Government.

The authors declare no competing financial interests.

Contributions: C.L. Lucas performed experiments, analyzed data, and developed and wrote the manuscript. Y. Zhang analyzed WES data and discovered *PIK3R1* mutations. A. Venida assisted with experiments and analyzed data. Y. Wang provided clinical care for and analysis of patient C.1. J. Hughes performed/organized WES studies and analyzed data. J. McElwee performed/organized WES studies and analyzed data. M. Butrick assisted with clinical management of patient A.1. H. Matthews assisted with clinical management of patients A.1, B.1, and B.II.1. S. Price assisted with clinical care of patient A.1. M. Biancalana performed structural modeling analyses. X. Wang provided clinical care for and supervised analysis of patient C.1. M. Richards provided clinical care for and evaluation of patient B.II.1. T. Pozos provided clinical care for and evaluation of patient B.II.1. I. Barlan provided clinical care for and evaluation of patient A.1. A. Ozen provided clinical care for and evaluation of patient A.1. V.K. Rao provided clinical care for and evaluation of patient A.1. H.C. Su provided clinical and research advice and supervised research and data analysis. M.J. Lenardo supervised research and data analysis, provided advice, and edited the manuscript. All authors discussed and reviewed the manuscript.

Submitted: 10 September 2014
Accepted: 20 November 2014

REFERENCES

Angulo, I., O. Vadas, F. Garçon, E. Banham-Hall, V. Plagnol, T.R. Leahy, H. Baxendale, T. Coulter, J. Curtis, C. Wu, et al. 2013. Phosphoinositide 3-kinase δ gene mutation predisposes to respiratory infection and airway damage. *Science*. 342:866–871. http://dx.doi.org/10.1126/science.1243292

Bárcena, C., V. Quesada, A. De Sandre-Giovannoli, D.A. Puente, J. Fernández-Toral, S. Sigaudy, A. Baban, N. Lévy, G. Velasco, and C. López-Otín. 2014. Exome sequencing identifies a novel mutation in PIK3R1 as the cause of SHORT syndrome. *BMC Med. Genet.* 15:51. http://dx.doi.org/10.1186/1471-2350-15-51

Brachmann, S.M., K. Ueki, J.A. Engelman, R.C. Kahn, and L.C. Cantley. 2005. Phosphoinositide 3-kinase catalytic subunit deletion and regulatory subunit deletion have opposite effects on insulin sensitivity in mice. *Mol. Cell. Biol.* 25:1596–1607. http://dx.doi.org/10.1128/MCB.25.5.1596-1607.2005

Brown, J.R., J.C. Byrd, S.E. Coutre, D.M. Benson, I.W. Flinn, N.D. Wagner-Johnston, S.E. Spurgeon, B.S. Kahl, C. Bello, H.K. Webb, et al. 2014. Idelalisib, an inhibitor of phosphatidylinositol 3-kinase p110δ, for relapsed/refractory chronic lymphocytic leukemia. *Blood*. 123:3390–3397. http://dx.doi.org/10.1182/blood-2013-11-535047

Burke, J.E., O. Vadas, A. Berndt, T. Finegan, O. Perisic, and R.L. Williams. 2011. Dynamics of the phosphoinositide 3-kinase p110δ interaction with p85α and membranes reveals aspects of regulation distinct from p110α. *Structure*. 19:1127–1137. http://dx.doi.org/10.1016/j.str.2011.06.003

Cancer Genome Atlas Research Network. 2008. Comprehensive genomic characterization defines human glioblastoma genes and core pathways. *Nature*. 455:1061–1068. http://dx.doi.org/10.1038/nature07385

Chudasama, K.K., J. Winnay, S. Johansson, T. Claudi, R. König, I. Haldorsen, B. Johansson, J.R. Woo, D. Aarskog, J.V. Sagen, et al. 2013. SHORT syndrome with partial lipodystrophy due to impaired phosphatidylinositol 3 kinase signaling. *Am. J. Hum. Genet.* 93:150–157. http://dx.doi.org/10.1016/j.ajhg.2013.05.023

Conley, M.E., A.K. Dobbs, A.M. Quintana, A. Bosompem, Y.D. Wang, E. Coustan-Smith, A.M. Smith, E.E. Perez, and P.J. Murray. 2012. Agammaglobulinemia and absent B lineage cells in a patient lacking the p85α subunit of PI3K. *J. Exp. Med.* 209:463–470.

Crank, M.C., J.K. Grossman, S. Moir, S. Pittaluga, C.M. Buckner, L. Kardava, A. Agharahimi, H. Meuwissen, J. Stoddard, J. Niemela, et al. 2014. Mutations in PIK3CD can cause hyper IgM syndrome (HIGM) associated with increased cancer susceptibility. *J. Clin. Immunol.* 34:272–276. http://dx.doi.org/10.1007/s10875-014-0012-9

Deau, M.C., L. Heurtier, P. Frange, F. Suarez, C. Bole-Feysot, P. Nitschke, M. Cavazzana, C. Picard, A. Durandy, A. Fischer, and S. Kracker. 2014. A human immunodeficiency caused by mutations in the PIK3R1 gene. *J. Clin. Invest.* 124:3923–3928. http://dx.doi.org/10.1172/JCI75746

Dhand, R., K. Hara, I. Hiles, B. Bax, I. Gout, G. Panayotou, M.J. Fry, K. Yonezawa, M. Kasuga, and M.D. Waterfield. 1994. PI 3-kinase: structural and functional analysis of intersubunit interactions. *EMBO J.* 13:511–521.

Dyment, D.A., A.C. Smith, D. Alcantara, J.A. Schwartzentruber, L. Basel-Vanagaite, C.J. Curry, I.K. Temple, W. Reardon, S. Mansour, M.R. Haq, et al. FORGE Canada Consortium. 2013. Mutations in PIK3R1 cause SHORT syndrome. *Am. J. Hum. Genet.* 93:158–166. http://dx.doi.org/10.1016/j.ajhg.2013.06.005

Flinn, I.W., B.S. Kahl, J.P. Leonard, R.R. Furman, J.R. Brown, J.C. Byrd, N.D. Wagner-Johnston, S.E. Coutre, D.M. Benson, S. Peterman, et al. 2014. Idelalisib, a selective inhibitor of phosphatidylinositol 3-kinase-δ, as therapy for previously treated indolent non-Hodgkin lymphoma. *Blood*. 123:3406–3413. http://dx.doi.org/10.1182/blood-2013-11-538546

Fruman, D.A., F. Mauvais-Jarvis, D.A. Pollard, C.M. Yballe, D. Brazil, R.T. Bronson, C.R. Kahn, and L.C. Cantley. 2000. Hypoglycaemia, liver necrosis and perinatal death in mice lacking all isoforms of phosphoinositide 3-kinase p85α. *Nat. Genet.* 26:379–382. http://dx.doi.org/10.1038/81715

Geering, B., P.R. Cutillas, G. Nock, S.I. Gharbi, and B. Vanhaesebroeck. 2007a. Class IA phosphoinositide 3-kinases are obligate p85-p110 heterodimers. *Proc. Natl. Acad. Sci. USA*. 104:7809–7814. http://dx.doi.org/10.1073/pnas.0700373104

Geering, B., P.R. Cutillas, and B. Vanhaesebroeck. 2007b. Regulation of class IA PI3Ks: is there a role for monomeric PI3K subunits? *Biochem. Soc. Trans.* 35:199–203. http://dx.doi.org/10.1042/BST0350199

Gilbert, J.A. 2014. Idelalisib: targeting PI3Kδ in B-cell malignancies. *Lancet Oncol.* 15:e108. http://dx.doi.org/10.1016/S1470-2045(14)70052-X

Jaiswal, B.S., V. Janakiraman, N.M. Kljavin, S. Chaudhuri, H.M. Stern, W. Wang, Z. Kan, H.A. Dbouk, B.A. Peters, P. Waring, et al. 2009. Somatic mutations in p85α promote tumorigenesis through class IA PI3K activation. *Cancer Cell*. 16:463–474. http://dx.doi.org/10.1016/j.ccr.2009.10.016

Kahl, B.S., S.E. Spurgeon, R.R. Furman, I.W. Flinn, S.E. Coutre, J.R. Brown, D.M. Benson, J.C. Byrd, S. Peterman, Y. Cho, et al. 2014. A phase 1 study of the PI3Kδ inhibitor idelalisib in patients with relapsed/refractory mantle cell lymphoma (MCL). *Blood*. 123:3398–3405. http://dx.doi.org/10.1182/blood-2013-11-537555

Keppler-Noreuil, K.M., J.C. Sapp, M.J. Lindhurst, V.E. Parker, C. Blumhorst, T. Darling, L.L. Tosi, S.M. Huson, R.W. Whitehouse, E. Jakkula, et al. 2014. Clinical delineation and natural history of the PIK3CA-related overgrowth spectrum. *Am. J. Med. Genet. A.* 164:1713–1733. http://dx.doi.org/10.1002/ajmg.a.36552

Kracker, S., J. Curtis, M.A. Ibrahim, A. Sediva, J. Salisbury, V. Campr, M. Debré, J.D. Edgar, K. Imai, C. Picard, et al. 2014. Occurrence of B-cell lymphomas in patients with activated phosphoinositide 3-kinase δ syndrome. *J. Allergy Clin. Immunol.* 134:233–236: 236.e3. http://dx.doi.org/10.1016/j.jaci.2014.02.020

Lannutti, B.J., S.A. Meadows, S.E. Herman, A. Kashishian, B. Steiner, A.J. Johnson, J.C. Byrd, J.W. Tyner, M.M. Loriaux, M. Deininger, et al. 2011. CAL-101, a p110δ selective phosphatidylinositol-3-kinase inhibitor for the treatment of B-cell malignancies, inhibits PI3K signaling and cellular viability. *Blood*. 117:591–594. http://dx.doi.org/10.1182/blood-2010-03-275305

Lee, J.H., M. Huynh, J.L. Silhavy, S. Kim, T. Dixon-Salazar, A. Heiberg, E. Scott, V. Bafna, K.J. Hill, A. Collazo, et al. 2012. De novo somatic mutations in components of the PI3K-AKT3-mTOR pathway cause hemimegalencephaly. *Nat. Genet.* 44:941–945. http://dx.doi.org/10.1038/ng.2329

Lindhurst, M.J., V.E. Parker, F. Payne, J.C. Sapp, S. Rudge, J. Harris, A.M. Witkowski, Q. Zhang, M.P. Groeneveld, C.E. Scott, et al. 2012. Mosaic overgrowth with fibroadipose hyperplasia is caused by somatic activating mutations in PIK3CA. *Nat. Genet.* 44:928–933. http://dx.doi.org/10.1038/ng.2332

Lucas, C.L., H.S. Kuehn, F. Zhao, J.E. Niemela, E.K. Deenick, U. Palendira, D.T. Avery, L. Moens, J.L. Cannons, M. Biancalana, et al. 2014. Dominant-activating germline mutations in the gene encoding the PI(3)K catalytic subunit p110δ result in T cell senescence and human immunodeficiency. *Nat. Immunol.* 15:88–97. http://dx.doi.org/10.1038/ni.2771

Mauvais-Jarvis, F., K. Ueki, D.A. Fruman, M.F. Hirshman, K. Sakamoto, L.J. Goodyear, M. Iannacone, D. Accili, L.C. Cantley, and C.R. Kahn. 2002. Reduced expression of the murine p85α subunit of phosphoinositide 3-kinase improves insulin signaling and ameliorates diabetes. *J. Clin. Invest.* 109:141–149. http://dx.doi.org/10.1172/JCI0213305

Parsons, D.W., S. Jones, X. Zhang, J.C. Lin, R.J. Leary, P. Angenendt, P. Mankoo, H. Carter, I.M. Siu, G.L. Gallia, et al. 2008. An integrated genomic analysis of human glioblastoma multiforme. *Science*. 321:1807–1812. http://dx.doi.org/10.1126/science.1164382

Rivière, J.B., G.M. Mirzaa, B.J. O'Roak, M. Beddaoui, D. Alcantara, R.L. Conway, J. St-Onge, J.A. Schwartzentruber, K.W. Gripp, S.M. Nikkel, et al. Finding of Rare Disease Genes (FORGE) Canada Consortium. 2012. De novo germline and postzygotic mutations in AKT3, PIK3R2 and PIK3CA cause a spectrum of related megalencephaly syndromes. *Nat. Genet.* 44:934–940. http://dx.doi.org/10.1038/ng.2331

Sun, M., P. Hillmann, B.T. Hofmann, J.R. Hart, and P.K. Vogt. 2010. Cancer-derived mutations in the regulatory subunit p85α of phosphoinositide 3-kinase function through the catalytic subunit p110α. *Proc. Natl. Acad. Sci. USA*. 107:15547–15552. http://dx.doi.org/10.1073/pnas.1009652107

Thauvin-Robinet, C., M. Auclair, L. Duplomb, M. Caron-Debarle, M. Avila, J. St-Onge, M. Le Merrer, B. Le Luyer, D. Héron, M. Mathieu-Dramard, et al. 2013. PIK3R1 mutations cause syndromic insulin resistance with lipoatrophy. *Am. J. Hum. Genet.* 93:141–149. http://dx.doi.org/10.1016/j.ajhg.2013.05.019

Ueki, K., D.A. Fruman, S.M. Brachmann, Y.H. Tseng, L.C. Cantley, and C.R. Kahn. 2002. Molecular balance between the regulatory and catalytic subunits of phosphoinositide 3-kinase regulates cell signaling and survival. *Mol. Cell. Biol.* 22:965–977. http://dx.doi.org/10.1128/MCB.22.3.965-977.2002

Ueki, K., D.A. Fruman, C.M. Yballe, M. Fasshauer, J. Klein, T. Asano, L.C. Cantley, and C.R. Kahn. 2003. Positive and negative roles of p85α and p85β regulatory subunits of phosphoinositide 3-kinase in insulin signaling. *J. Biol. Chem.* 278:48453–48466. http://dx.doi.org/10.1074/jbc.M305602200

Urick, M.E., M.L. Rudd, A.K. Godwin, D. Sgroi, M. Merino, and D.W. Bell. 2011. PIK3R1 (p85α) is somatically mutated at high frequency in primary endometrial cancer. *Cancer Res.* 71:4061–4067. http://dx.doi.org/10.1158/0008-5472.CAN-11-0549

Vanhaesebroeck, B., K. Ali, A. Bilancio, B. Geering, and L.C. Foukas. 2005. Signalling by PI3K isoforms: insights from gene-targeted mice. *Trends Biochem. Sci.* 30:194–204. http://dx.doi.org/10.1016/j.tibs.2005.02.008

Wong, K.K., J.A. Engelman, and L.C. Cantley. 2010. Targeting the PI3K signaling pathway in cancer. *Curr. Opin. Genet. Dev.* 20:87–90. http://dx.doi.org/10.1016/j.gde.2009.11.002

Yu, J., Y. Zhang, J. McIlroy, T. Rordorf-Nikolic, G.A. Orr, and J.M. Backer. 1998. Regulation of the p85/p110 phosphatidylinositol 3′-kinase: stabilization and inhibition of the p110α catalytic subunit by the p85 regulatory subunit. *Mol. Cell. Biol.* 18:1379–1387.

Zhao, J.J., H. Cheng, S. Jia, L. Wang, O.V. Gjoerup, A. Mikami, and T.M. Roberts. 2006. The p110α isoform of PI3K is essential for proper growth factor signaling and oncogenic transformation. *Proc. Natl. Acad. Sci. USA*. 103:16296–16300. http://dx.doi.org/10.1073/pnas.0607899103